

# RHanDS: Refining Malformed Hands for Generated Images with Decoupled Structure and Style Guidance

Chengrui Wang\*  
wangchengrui.wcr@alibaba-inc.com  
Alibaba Group  
Beijing, China

Pengfei Liu\*  
pengfei@stu.xmu.edu.cn  
Xiamen University  
Xiamen, China

Min Zhou  
yunqi.zm@alibaba-inc.com  
Alibaba Group  
Beijing, China

Ming Zeng†  
zengming@stu.xmu.edu.cn  
Xiamen University  
Xiamen, China

Xubin Li  
lxb204722@alibaba-inc.com  
Alibaba Group  
Beijing, China

Tiezheng Ge  
Bo zheng  
tiezheng.gt@alibaba-inc.com  
bozheng@alibaba-inc.com  
Alibaba Group  
Beijing, China

## ABSTRACT

Although diffusion models can generate high-quality human images, their applications are limited by the instability in generating hands with correct structures. Some previous works mitigate the problem by considering hand structure yet struggle to maintain style consistency between refined malformed hands and other image regions. In this paper, we aim to solve the problem of inconsistency regarding hand structure and style. We propose a conditional diffusion-based framework RHanDS to refine the hand region with the help of decoupled structure and style guidance. Specifically, the structure guidance is the hand mesh reconstructed from the malformed hand, serving to correct the hand structure. The style guidance is a hand image, e.g., the malformed hand itself, and is employed to furnish the style reference for hand refining. In order to suppress the structure leakage when referencing hand style and effectively utilize hand data to improve the capability of the model, we build a multi-style hand dataset and introduce a two-stage training strategy. In the first stage, we use paired hand images for training to generate hands with the same style as the reference. In the second stage, various hand images generated based on the human mesh are used for training to enable the model to gain control over the hand structure. We evaluate our method and counterparts on the test dataset of the proposed multi-style hand dataset. The experimental results show that RHanDS can effectively refine hands structure- and style- correctly compared with previous methods. The codes and datasets will be available soon.

## KEYWORDS

malformed hand refining, diffusion models, conditional generation

## 1 INTRODUCTION

Text-to-image diffusion models [24, 26, 28, 29, 33] have exhibited the remarkable ability to synthesize visually stunning images based on textual prompts, representing a significant advancement in image generation. Despite their impressive capabilities, current models still face challenges in effectively handling intricate structures like

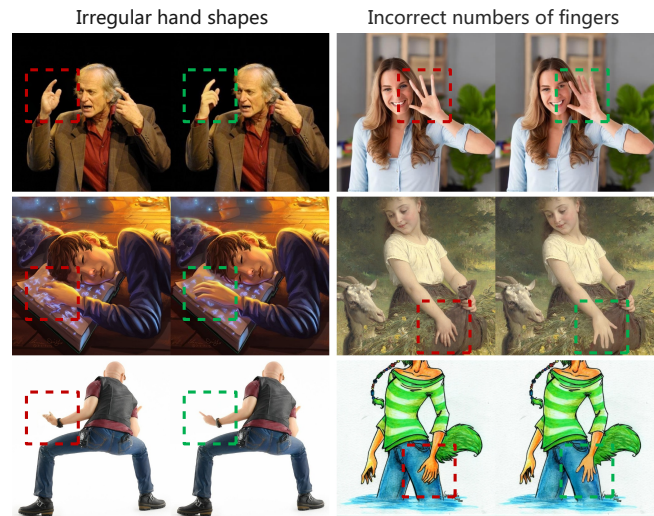


**Figure 1: Examples of hands refined by our RHanDS (right in each pair) from malformed hand (left in each pair). Typical malformations of generated hands include irregular hand shapes and incorrect numbers of fingers.**

hands [26, 29]. As illustrated in Figure 1, models often produce malformed hands with irregular shapes or incorrect numbers of fingers, deviating from the realistic 3D shape and physical limitations of human hands.

To solve the problem, Lu *et al.* [20] introduces a post-processing solution that employs an inpainting diffusion model to refine the malformed hand in the generated image. During the inpainting process, a 3D hand mesh is reconstructed based on the malformed hand image, rendered as a depth image to provide structural guidance for correcting the malformed hand through ControlNet [40]. This inpainting method, which incorporates hand structure control, indeed effectively enhances the structural accuracy of generating hand images. However, the generated hand image may lack consistency in color, texture, and other stylistic features compared to the original malformed hands, resulting in a lack of harmony

\*Both authors contributed equally to the paper

†Corresponding author

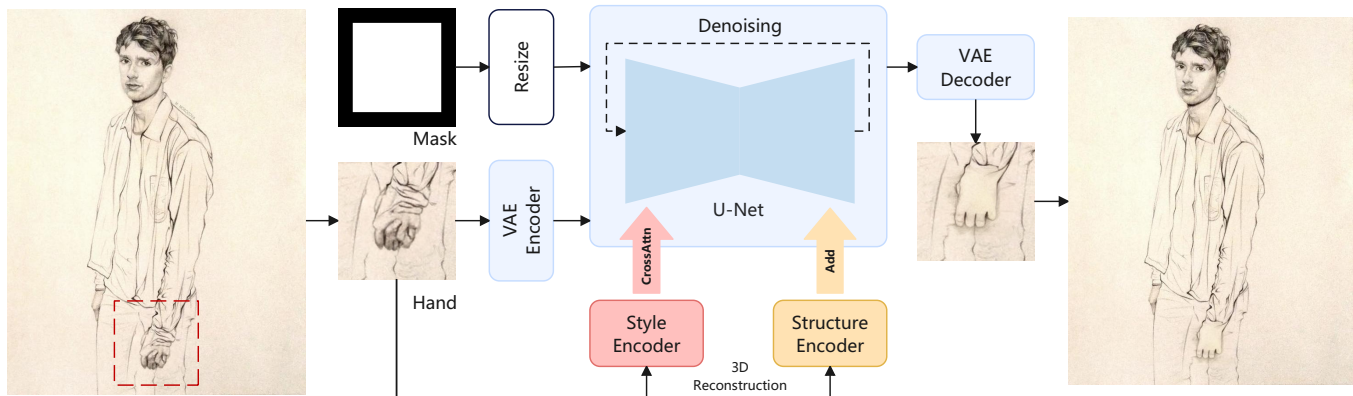


**Figure 2: The RHandDS framework we propose contains four modules: a VAE for projecting images into a latent space and reconstructing images from the latent, a conditional U-net for predicting the denoised variant during the denoising process, a style encoder to extract hand style from the malformed hand and map it into the U-net via cross-attention, and a structure encoder to utilize the hand mesh reconstructed from the malformed hand to guide the hand structure. In addition, to achieve a fully automatic process, a hand detection model and a 3D hand reconstruction model are required.**

with the overall image. This issue will become more serious when dealing with hand styles that are less common in datasets, such as in sculpture or cartoon images. It may be due to the indirect access to hand style information, requiring implicit inference of hand texture and color from other skin areas in the image during the inpainting process. In order to alleviate this phenomenon, it is intuitive to consider utilizing the image region of the original malformed hand to enhance style consistency. However, it remains an open challenge to selectively incorporate hand style features without introducing structural information [37], in order to avoid interference with the correct hand structure.

In this paper, we propose a novel framework named RHandDS to Refine malformed Hands with Decoupled Structure and Style guidance, which is adapted to malformed hands of arbitrary styles. As shown in Figure 2, RHandDS repaints the hand region based on diffusion models to refine the malformed hand structure while preserving the hand style. Specifically, RHandDS utilizes the 3D mesh reconstructed from the malformed hand for structural guidance via the rendered depth image and structure encoder, and uses the style encoder to extract the style embedding from the malformed hand for style guidance.

In order to suppress the leakage of hand structure from style embedding, we also introduce a two-stage training strategy and propose corresponding hand datasets. The purpose of the first-stage training is to equip the model with the capability of repainting hands with a given style. In order to extract hand styles while ignoring structural information, we collect a large number of realistic image pairs depicting the left and right hands of the same person (i.e., images that share the same style but exhibit different structures). We then use one hand as a style reference to guide the generation of the other hand. In this stage, we only train the style encoder and U-net, with the structure encoder remaining uninitialized. In the second stage, our objective shifts towards making the model generate hand images with additional structural control. Considering the limited style diversity in existing hand image datasets (with

3D meshes, data like these are called as hand-mesh pairs for convenience in this paper), we propose a novel approach using the SMPL model and ControlNet to create a more diverse dataset. We initiate this process by generating hand meshes using the SMPL model and rendering the corresponding depth images. ControlNet is then utilized to generate hand images, controlled with depth images and prompts indicating various style categories. The generated hand images are evaluated by calculating the Mean Per Joint Position Error (MPJPE) [16] metric. Images with small MPJPE differences are deemed to have higher structural accuracy and are retained for training the structure encoder while maintaining the network’s other parameters unchanged.

Besides, to verify the hand refining ability, we use a standard diffusion model to regenerate the hand regions in the HumanArt dataset [17], and propose a multi-style malformed hand dataset with mesh-image pairs for evaluation. Qualitative and quantitative experiments show the effectiveness and superiority of RHandDS.

In summary, the contributions of this work are as follows:

- For refining malformed hand images, we propose a novel framework named RHandDS with decoupled structure and style guidance. Benefiting from direct and decoupled style guidance for malformed hands, our model can maintain stylistic consistency before and after hand refining and generate hand images in diverse styles.
- We propose a two-stage training strategy and create corresponding datasets, which effectively enable the model to learn control over hand style and hand structure separately.
- Experiments show that RHandDS can effectively handle malformed hands in various styles and restore them to better structures.

## 2 RELATED WORK

### 2.1 Diffusion Models for Image Synthesis

Recent advancements have been greatly promoted by text-to-image diffusion models. Specifically, the technique of Latent Diffusion

Models (LDM) [29] conducts diffusion in a latent image space [35], which largely reduces computational demands. Stable Diffusion [3] is one of the highlighted works of LDM, which utilizes a pre-trained language encoder like CLIP [27] to encode the text prompt into latent space to guide the diffusion process.

Diverging from the text-to-image paradigm, image inpainting is tasked with synthesizing visually plausible content within the masked regions of the existing image, ensuring that the synthesized content maintains semantic coherence with the context of the unmasked regions. By fine-tuning the pre-trained text-to-image Stable Diffusion model, the specialized variant known as Stable Diffusion Inpainting [2] can synthesize content within the masked region that follows textual prompts. However, fine-grained control over the structure and style of the inpainting contents cannot be achieved solely through text guidance.

In order to provide fine-grained conditions during the generation process, different control methods have been explored in previous studies, and it has been demonstrated that an additional module can be effectively plugged into the existing diffusion models to guide the image generation. ControlNet [40] and T2I-Adapter [23] use spatial conditions such as canny, depth images, and body poses as inputs to control the structure of the generated image. In order to reduce the fine-tuning cost, Uni-ControlNet [41] allows for the simultaneous utilization of different conditions within one single model. Previous subject-driven approaches such as DreamBooth [32], Textual Inversion [7], LoRA [14], and Concept Sliders [8] achieved stylization and customization by fine-tuning parameters. In contrast, IP-Adapter [37] leverages pre-trained image encoder [27] to achieve the image prompt capability for diffusion models, generating images that resemble the reference images in content and style.

## 2.2 Plausible Hand Generation

Concept Sliders [8] use parameter-efficient training method [14] to learn better physical structure of hand by fine-tuning diffusion models with carefully selected data. Yeet *al.* [38] synthesize hand-object interaction on existing images using the rough region of the palm and forearm as guidance. However, the inherent complex structure of 3D human hands makes it difficult for these methods to generate correct hands stably. Different from the methods that directly generate hands, some works [20, 36, 38] introduce the structure information of the target hand into a model to prevent the model from generating malformed hands. HanDiffuser [38] encodes the 3D hand parameters into text embedding for achieving text-to-image generation with realistic hand appearances. Diffusion-HPC [36] proposes a post-processing method that refines the generated malformed person through a conditional diffusion model with the help of a human depth image rendered based on the reconstructed human mesh. HandRefiner [20] proposes a similar post-processing method more suitable for dealing with malformed hands.

Our RHanDS is a post-processing method that leverages 3D hand mesh as the pixel-level condition to control hand structure. Compared to existing methods, RHanDS performs specifically on the hand region rather than the entire image, which facilitates more precise refinement. Moreover, RHanDS enhances the perception of hand style, ensuring that the style of the refined hand seamlessly

aligns with that of the original image for a coherent and authentic representation.

## 3 METHODOLOGY

Given a generated image that contains malformed human hands, we aim to correct the structure of the malformed hand. To this end, in this section, we introduce the detail of our proposed diffusion-based framework *RHanDS*. As shown in Figure 2, RHanDS mainly contains four modules: style encoder  $\mathcal{E}_{style}$ , structure encoder  $\mathcal{E}_{struc}$ , U-net  $\epsilon_\theta$  and VAE  $\mathcal{E}$  and  $\mathcal{D}$ . Specifically, the inputs of the whole framework are a cropped malformed hand image  $x$ , a structure reference  $ref_{struc}$ , a style reference  $r_{style}$ , and a mask  $mask$ . The malformed hand image  $x$  is cropped out from the entire image for effective refining. The structure reference  $ref_{struc}$  is a hand depth image rendered from a hand model that can be manually created using 3D tools [42] or automatically obtained from the 3D mesh reconstructed from malformed hand and is encoded by the structure encoder  $\mathcal{E}_{struc}$  to guide the hand structure. The style reference  $r_{style}$  is a hand image that can either be the malformed hand itself or any other hand image and is encoded by the style encoder  $\mathcal{E}_{style}$  to guide the hand style. The binary mask  $mask$  indicates the malformed hand region that needs to be repainted. The overall training process is decomposed into two stages to decouple the structure and style guidance. In the first stage (Section 3.2), U-net and style encoder are trained using multi-style paired hand images. In the second stage (Section 3.3), the structure encoder is trained using the multi-style hand-mesh dataset.

Our RHanDS ensures the correctness of the structure with a 3D hand model, maintains the correctness of the style with reference hands, and avoids the mutual influence that exists between structure and style guidance. As a result, RHanDS can produce plausible hand images  $x'$  with the correct structure while preserving the hand style.

### 3.1 Preliminaries

RHanDS is built on top of stable diffusion, which performs the diffusion process efficiently in the latent space rather than pixel space. Specifically, given an image  $x_0$  in RGB space, the encoder  $\mathcal{E}$  first encodes the image into a latent representation  $z_0 = \mathcal{E}(x_0)$ . During the forward process, normally-distributed noise  $\epsilon_t$  is added into the latent  $z_0$  to obtain the noisy latent  $z_t$ . During the reverse process, the stable diffusion model implements denoising U-net  $\epsilon_\theta$  as the backbone to predict the noise  $\epsilon_t$  with noisy latent  $z_t$  and current timestep  $t$ . The simple training objective can be written as

$$\mathcal{L} = \mathbb{E}_{z_0, \epsilon \sim \mathcal{N}(0,1), t} [\|\epsilon - \epsilon_\theta(z_t, t)\|_2^2]. \quad (1)$$

To correct the structure of malformed hand in image while keeping other region unchanged, the underlying neural backbone of RHanDS is implemented as the U-net of stable diffusion inpainting model, a particular variant of stable diffusion, which enables the functionality of inpainting specified regions of an image under the guidance of a mask. Compared to the standard version of stable diffusion, this U-net has five additional input channels for supporting inpainting. Specifically, four of these channels are allocated for the encoded masked-image  $\hat{z}_0$ , while the remaining single channel is allocated for the resized mask  $mask$ . During reverse process, the U-net predicts the noise through  $\epsilon_t = \epsilon_\theta(z_t, \hat{z}_0, mask, t)$  while  $\hat{z}_0$

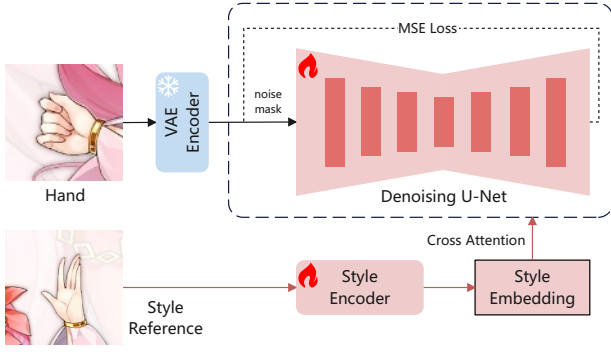


**Figure 3: The first-stage training of RHandS. In this stage, U-net and style encoder are trained using multi-style paired hand images for style guidance.**

and *mask* keep unchanged. After the reverse process, the decoder  $\mathcal{D}$  reconstructs the image from the latent.

### 3.2 The First Stage: Style Guidance

As shown in Figure 6, the existing solutions are limited in the perception of hand style and exhibit poor generalization ability in images with anime, oil painting, watercolor, and other styles. To solve the problem, we have to encode the hand style into U-net, enabling the model to refine hands  $x$  based on style reference  $r_{style}$ . Similar to the approach used in IP-Adapter [37], we use a CLIP [27] image encoder to extract the image embedding from  $r_{style}$ . To enforce the CLIP model extract styles from hand images without introducing other extraneous information such as hand structure, we choose the global image embedding and use a linear projection network to transform the image embedding into a sequence of features with length *tokens* to obtain the style embedding  $c_{style}$ . Overall, the style encoder  $\mathcal{E}_{style}$  consists of a CLIP image encoder and a linear projection network, and style embedding  $c_{style}$  that can be formulated as follows:

$$c_{style} = \mathcal{E}_{style}(r_{style}) \quad (2)$$

As the style embedding already contains sufficient information for hand refining, we drop the text features and directly feed the style embedding into U-net through cross-attention layers. Given the style embedding, the output of cross-attention  $\mathbf{Z}$  is computed as follows:

$$\mathbf{Z} = \text{Attention}(\mathbf{Q}, \mathbf{K}, \mathbf{V}) = \text{Softmax}\left(\frac{\mathbf{Q}\mathbf{K}^T}{\sqrt{d}}\right)\mathbf{V}, \quad (3)$$

where  $\mathbf{Q} = \mathbf{Z}\mathbf{W}_q$ ,  $\mathbf{K} = c_{style}\mathbf{W}_k$ ,  $\mathbf{V} = c_{style}\mathbf{W}_v$  are query, key, value matrices of the attention layer respectively, and  $\mathbf{W}_q$ ,  $\mathbf{W}_k$ ,  $\mathbf{W}_v$  are the weight matrices of the linear projection layers in attention module.

As shown in Figure 3, in this stage, we train the U-net and the style encoder on the dataset with multi-style paired hands, using the same training objective as stable diffusion:

$$\mathcal{L} = \mathbb{E}_{z_t, \epsilon, t} [\|\epsilon - \epsilon_\theta(z_t, c_{style}, \text{mask}, t)\|_2^2]. \quad (4)$$

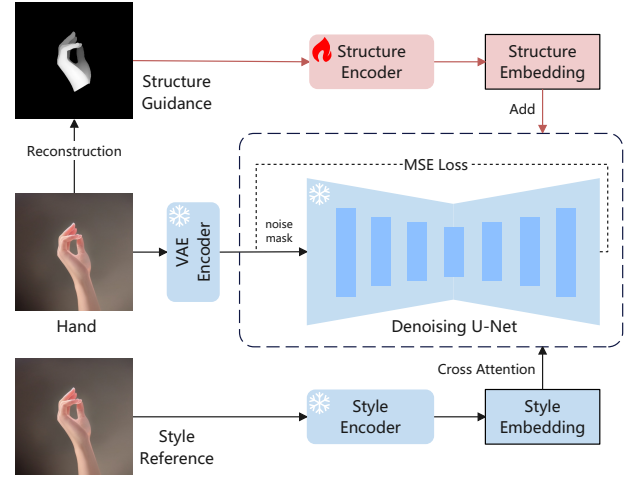


**Figure 4: The second-stage training of RHandS. In this stage, structure encoder is trained using multi-style hand-mesh data for structure guidance.**

where  $c_{style}$  used to supply style guidance is encoded from one hand image, and  $z_0$  used for training U-net to predict noise is encoded from the other hand image  $x$ . It is worth noting that  $r_{style}$  needs to be different from  $x$  in terms of gesture while maintaining consistency in hand style, and the  $r_{style}$  and  $x$  must exhibit diversity in styles. Otherwise, the style encoder  $\mathcal{E}_{style}$  would encode the gesture of the  $r_{style}$  for noise prediction or fail to encode style guidance for U-net. To build the multi-style paired hand dataset that meets the requirements, we crop the two hands of the same character that exhibit the same style but different gesture from the characters images of varying styles. The details of this dataset can be found in Subsection 4.1.

### 3.3 The Second Stage: Structure Guidance

With the assistance of the style encoder, our framework can utilize the style reference  $r_{style}$  to guide the refining process of malformed hands. However, as shown in Figure 6, it is hard to correct the structure of the malformed hand stably due to the inherent complex structure of 3D human hands. To solve the problem, we adopt MANO [30], a 3D hand model with articulated and non-rigid deformations, to represent the correct gesture and structure of hands. Specifically, we used MANO-based methods to reconstruct the 3D hand mesh from the malformed hand image. For malformed hands that are difficult to reconstruct automatically, this process can also be completed manually using existing tools [42]. The correct hand structure has been determined by the 3D hand mesh, and following [20], we render the hand depth image from the hand mesh as structure reference  $r_{struc}$  to guide the correction of hand structure.

To encode the structure reference  $r_{struc}$  into U-net for structure guidance, we use the structure encoder  $\mathcal{E}_{struc}$  to encode the structure reference  $r_{struc}$ , and  $\mathcal{E}_{struc}$  adopts the same structure as ControlNet [40]. Different from the original setting in [40], we feed a learnable embedding  $c_l$  into the cross-attention layers of  $\mathcal{E}_{struc}$  to maintain the performance of pre-trained model. Specially, the

input of  $\mathcal{E}_{struc}$  is consist of structure reference  $r_{struc}$ , noisy latent  $z_t$  and learnable embedding  $c_l$ . The output of  $\mathcal{E}_{struc}$  is the structure embedding  $c_{struc}$  that can be formulated as follows:

$$c_{struc} = \mathcal{E}_{struc}(r_{struc}, z_t, c_l) \quad (5)$$

For all the outputs  $out^i$  of the middle block and decoder blocks of U-net, the structure embedding  $c_{struc}^i$  is fed into U-net through a  $1 \times 1$  convolution layer  $\mathbb{Z}^i$  with structure weight  $w$ :

$$out^i = out^i + w \cdot \mathbb{Z}^i(c_{struc}^i) \quad (6)$$

As shown in Figure 4, in this stage, we freeze the U-net and the style encoder to maintain the capability of style guidance, and train the structure encoder on the multi-style hand-mesh dataset, using the training objective as follows:

$$\mathcal{L} = \mathbb{E}_{z_t, \epsilon, t} [\|\epsilon - \epsilon_{\theta}(z_t, c_{style}, c_{struc}, mask, t)\|_2^2]. \quad (7)$$

where  $c_{style}$  and  $z_0$  are encoded from the same hand image, and  $c_{struc}$  is encoded from the hand depth image obtained by rendering the 3D hand mesh. However, the model tends to overfit the hand styles present in the dataset due to style limitations inherent within the existing hand-mesh dataset [1, 5, 43]. A potential solution is to employ a depth estimation model [4] to predict hand depth from multi-style hand datasets, but the noise inherent in the depth prediction may undermine the capability to control hand structure. Based on the depth-controlled text-to-image generation pipeline, we use stable diffusion and ControlNet to create a multi-style hand-mesh dataset by using the depth image rendered from random hand meshes. The details of this dataset can be found in Section 4.2.

## 4 MULTI-STYLE DATASET

We have introduced a hand-refining model that decouples style and structure, along with a two-stage training strategy. In this section, we will introduce a series of datasets purposefully constructed for this method. As shown in Figure 5, Multi-Style Hand Dataset and Multi-Style Hand-Mesh Dataset correspond to the two stages of training, while Multi-Style Malformed Hand-Mesh Dataset serves as the test set. They encompass various data types and styles of hands. Detailed information about these datasets is provided below.

### 4.1 Multi-Style Paired Hand Dataset

During the first-stage training, to enable the model to refine hands under style guidance while preventing the leakage of hand structure, we propose a dataset consisting of hand pairs in a variety of styles, with each pair having the same style but different gestures. We find these pairs by detecting the different hands of one person. Specifically, we employ the YOLOv8 [34] to detect human hands and use [6] to detect human pose, which allows us to filter out hands belonging to the same person. This dataset includes 517,096 hand pairs from natural human images that are various in texture, and 2,423 hand pairs from anime images.

### 4.2 Multi-Style Hand-Mesh Dataset

During the second-stage training, to prevent the model from overfitting to the generation of hands in a single style, we first utilize the SMPL model [19] to create hand meshes and get corresponding



**Figure 5: The multi-style datasets. *Multi-Style Paired Hand Dataset* includes hand images of both hands of characters. *Multi-Style Hand-Mesh Dataset* includes hand meshes and hand images generated based on meshes. *Multi-Style Malformed Hand-Mesh Dataset* includes real hands, malformed hands generated from real hands, and hand meshes reconstructed from real hands.**

depth images. Then, we employ the depth-conditioned ControlNet to generate multi-style hand images with text prompts indicating different style categories. We reconstruct the hand mesh from the generated hand images and calculate the MPJPE metric  $MPJPE(K, K') = \mathbb{E}\|K - K'\|$  to filter out poorly structured hands, where  $K, K'$  are the 2D projection coordinates of the hand joints, corresponding to the SMPL hand mesh and the reconstructed hand mesh. Ultimately, this dataset includes seven different style categories, with 8,000 hand-mesh pairs for each style.

### 4.3 Multi-Style Malformed Hand-Mesh Dataset

To evaluate the model's ability to handle multi-style hands, we extract hand images from the HumanArt [17] dataset and use stable diffusion to regenerate the hand regions by SDEdit [22]. For

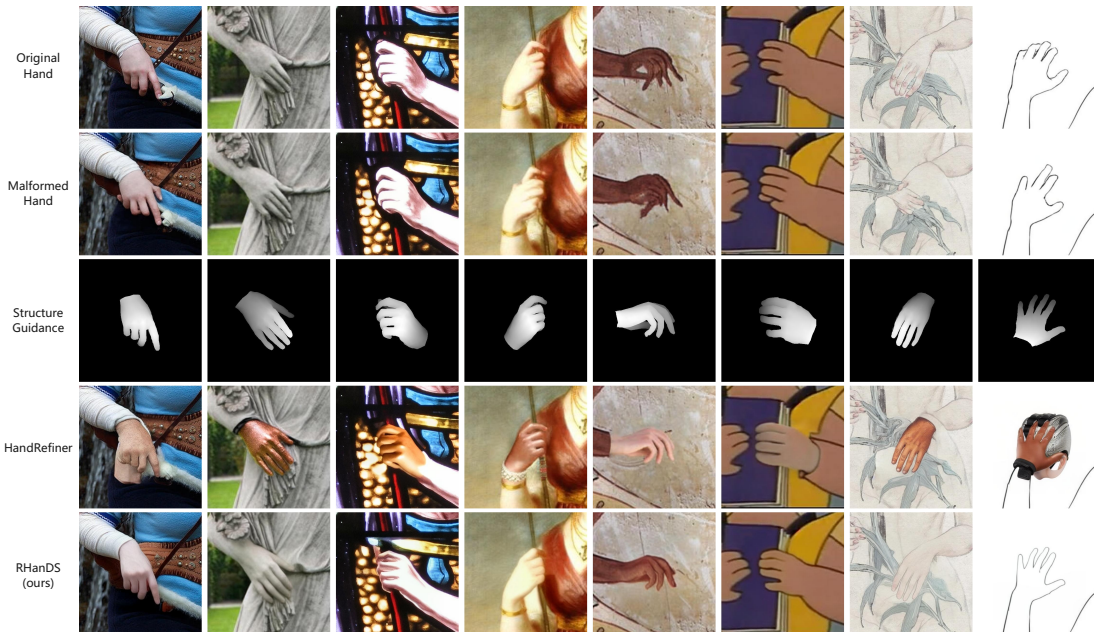


**Figure 6: The visual comparison of methods with other methods conditioned on different hand styles. The malformed hand is generated based on the original hand, and the structure guidance is reconstructed from the original hand. For our RHandS, *stage-1 only* denotes the model subjected to only the first stage of training, *stage-2 only* denotes the model trained entirely on the multi-style hand-mesh dataset, and *RHandS* denotes the model that has been fully trained through the two-stage training.**

evaluation, the style reference is the malformed hand itself, while the structure reference is reconstructed from the original hands using [5]. After filtering out the data with reconstruction failures, we collect 1440 pairs in total, consisting of natural styles and thirteen categories of artificial styles.

## 5 EXPERIMENTS

### 5.1 Implementation Details

In order to utilize the generation capability of existing model, the VAE and U-net of our RHandS are initialized from Stable Diffusion Inpainting v1.5, and the structure encoder is initialized from pre-trained depth ControlNet. For the style encoder, CLIP ViT-H/14 [15] is adopted as the image encoder, and the linear projection network is randomly initialized.

For the first stage, we use our Multi-Style Paired Hand Dataset to train U-net and style encoder for 15k iterations with a learning rate of  $1e-5$  and with a total batch size of 256 on 8 NVIDIA-A100 GPUs. The default token length  $token$  for the style encoder is set to 8. The hand images  $x$  are resized to  $512 \times 512$ , and the style references  $r_{style}$  are resized to  $224 \times 224$  with the processing of random horizontal and vertical flips.

For the second stage, we use the combination of Static Gesture Dataset [1] (SGD) and our Multi-Style Hand-Mesh Dataset to train structure encoder for 15k iterations with a learning rate of  $2e-5$  and with a total batch size of 256 on 8 NVIDIA-A100 GPUs. The weight  $w$  for the structure encoder is set to 1 during training. The structure references  $r_{struc}$  are resized to  $512 \times 512$ , and the depth values of the hand are normalized into  $[0.2, 1.0]$ .

Additionally, the mask  $mask$  we use to indicate the hand region covers the middle 9/16 of the entire image. In order to learn style guidance from the style encoder rather than the remaining skins in the image, we apply a strategy to randomly expand the region indicated by the mask to force the model to repaint all the skin in the image. Meanwhile, we randomly replace the style embedding with a learnable style embedding with a probability of 0.1 and set the mask to the entire image with a probability of 0.5. We adopt noise offset [10] and min-SNR strategy [11] for training.

During inference, we add the maximum (strength = 1.0) to image  $x$  and adopt DDPM [13] sampler for denoising. We use structure weight  $w = 0.6$ , denoising step  $steps = 25$  as default.

### 5.2 Evaluation Metrics

We use several metrics to evaluate the performances: (1) Fréchet Inception Distance [12] (FID) focuses on the overall distribution statistics of the refined images and the Ground Truth, (2) Style loss[9] evaluates the style consistency between the refined images and the Ground Truth, (3) MPJPE [16] between reconstructed 2D hand poses measures the structure consistency, (4) Keypoint detection confidence scores (Conf.) of a hand detector [21, 39] is used to indicate the plausibility of generated hands. The FID and style loss are calculated between the refined hands and the original hands. And the MPJPE is calculated between the reconstructed hand mesh and the structure reference, where the hand mesh is reconstructed from the refined hand using MobRecon [5]. By default, MPJPE is calculated based on the resolution of  $512 \times 512$ .

Method	Style Encoder	Structure Encoder	MPJPE ↓	Conf. ↑	FID ↓	Style Loss (×100) ↓
Malformed Dataset	-	-	40.29	0.86	23.84	2.77
HandRefiner	-	-	33.27	0.88	38.52	10.13
RHandS	stage-2	stage-2	26.29	0.89	47.76	7.11
RHandS	stage-1*	stage-2	29.48	0.88	33.68	5.35
RHandS	stage-1	stage-2*	<b>26.17</b>	<b>0.91</b>	33.56	5.23
<b>RHandS</b>	stage-1	stage-2	27.23	0.89	<b>32.59</b>	<b>5.04</b>

**Table 1: Quantitative comparison of the proposed RHandS with other methods on Multi-Style Malformed Hand-Mesh Dataset. stage-1\* denotes that one hand serves as both a style reference and hand image for the first stage training, and stage-2\* denotes that only using the SGD dataset for the second stage training.**

Method	FID ↓	MPJPE ↓	Conf. ↑
Text2Image Dataset			
Stable Diffusion†	77.60	-	0.93
HandRefiner†	74.12	-	0.94
RHandS†	<b>73.63</b>	-	0.94
Image2Image Dataset			
HandRefiner†	13.97	7.87	0.97
RHandS†	<b>13.54</b>	<b>6.89</b>	0.97
HandRefiner	33.84	12.02	0.94
RHandS	<b>22.18</b>	<b>9.86</b>	<b>0.96</b>

**Table 2: Quantitative comparison of the proposed RHandS with other methods on datasets [20]. The method with † represents calculating metrics on the entire image, while the method without † represents calculating metrics only on the hand region.**

### 5.3 Results and Comparison

We conducted a series of qualitative and quantitative analyses to verify the effectiveness of our method.

**Comparison between different methods on HandRefiner Dataset.** We evaluate our method on two datasets proposed by HandRefiner. The Text2Image Dataset includes 12K images generated with the text descriptions from HAGRID [18], and the Image2Image Dataset includes 2K images sampled from HAGRID. Following the setting in HandRefiner, for each image, we extract the hand region and refine the hand, then paste it back to the original image and calculate metrics on the entire image. Meanwhile, we found that calculating metrics on the hand region extracted using a fixed strategy can eliminate the influence of hand proportion and image size on the evaluation metrics. Therefore, we also report the metrics calculated on the hand region. As shown in Table 2, our RHandS outperform RandRefiner on both datasets.

**Comparison between different methods on Multi-Style Malformed Hand-Mesh Dataset.** According to the given settings, we use HandRefiner to refine the hands in our multi-style malformed hand-mesh dataset. As shown in Figure 6, the hands refined by HandRefiner are almost fixed in style, which is different from the original hand style. The quantitative experiments in Table 1 show that our RHandS outperforms HandRefiner in all metrics in terms of the style and structure of refined hands.

**Style-structure cross reference.** To verify the robustness and generalization of RHandS, we conducted experiments with various



**Figure 7: Visualization of hands generated under the guidance of different style and structure references.**

styles across different structure references. During inference, we mask the entire image to achieve the more intuitive result in Figure 7. Since the style and structure guidance are decoupled during training, we can generate hands with specified structures under any style reference without worrying about structure leakage.

### 5.4 Ablation Study

In this subsection, we will validate the effectiveness of the two-stage training strategy and dataset construction through quantitative experiments. Additionally, we will analyze the roles of the style and structure modules within the network.

**Effect of two-stage training.** Without the first-stage training, we train the entire model on the multi-style hand-mesh dataset with a single hand as both hand image  $x$  and style reference  $r_{ref}$ . As shown in Table 1, this model can achieve performance comparable to the two-stage training model in terms of MPJPE and Conf., but the FID has increased by 15.17, and the style loss has increased by 2.07. Meanwhile, compared with the model without structure encoder (FID 33.33, Style Loss 5.50), the FID is increased by 14.43 and the style loss is increased by 1.61. These demonstrate that the

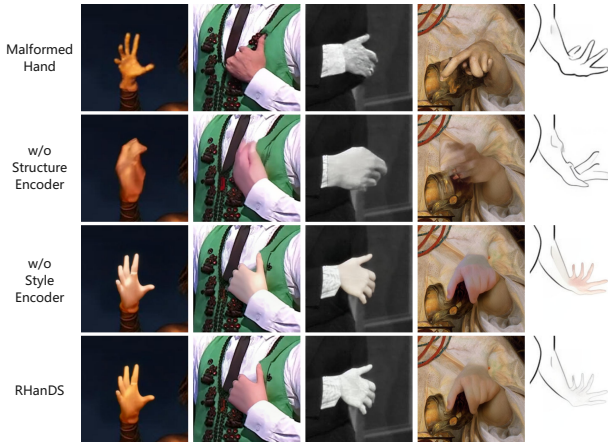


**Figure 8: The visual comparison of the effects of different modules.**

first-stage training is beneficial for helping the model perceive hand style from style reference.

**Effect of Paired Hand Dataset.** To clarify the impact of hand structure information leaked from the style encoder on hand refinement, we use the unpaired hands for the first stage training, where the style reference  $r_{ref}$  uses the same image as the hand image  $x$ . As shown in Table 1, the model trained with paired hands achieves better performance on all metrics, especially on the metrics related to hand structure.

**Effect of Multi-Style Hand-Mesh Dataset.** To clarify the role of multi-style hand-mesh data in two-stage training, we conduct an experiment using only the SGD dataset for the second-stage training. As shown in Table 1, compared with using both SGD and the multi-style hand-mesh dataset, the model trained with the SGD dataset outperformed in terms of MPJPE and Conf. by 1.06 and 0.02, respectively. The reason for better MPJPE and Conf. is that, unlike the hand images generated using stable diffusion in the multi-style hand-mesh dataset, the hand images rendered from mesh in SGD are more stable in hand structure. However, due to the low style diversity of hand data in SGD, the FID increased by 0.97, and the style loss increased by 0.19.

**Effects of different modules.** In RHandS, we use style encoders and structure encoders to guide the style and structure of the hands. To illustrate the effects of these two modules, we separately shield the structure encoder and the style encoder during inference. Specifically, we set the structure weight  $w$  to 0 to shield the structure encoder, and using the learnable style embedding rather than extract embedding from the style reference to shield the style encoder. Qualitative analysis in Figure 8 shows that the structure of the hand tends to be deformed without the structure encoder, and the style of the hand is easily changed without the style encoder.

**Structure weights.** The structure weight  $w$  is adjustable during inference. As shown in Table 3, the optimal value of structure weight is almost in the range of 0.4 to 0.6. Specifically, we choose the setting of  $w = 0.6$  as optimal. This setting achieves the best MPJPE and Conf., which is important in controlling hand structure.

$w$	MPJPE ↓	Conf. ↑	FID ↓	Style Loss ( $\times 100$ ) ↓
0.0	67.19	0.833	33.33	5.50
0.2	48.32	0.867	31.50	4.96
0.4	31.50	0.895	<b>31.20</b>	<b>4.71</b>
0.6	<b>27.23</b>	<b>0.896</b>	32.59	5.04
0.8	27.29	0.891	34.46	5.62
1.0	29.73	0.881	37.46	6.22

**Table 3: Ablation study on the impact of structure weight  $w$ .**



**Figure 9: Failure examples. The first row is the malformed hands, the second row is the hands refined by our RHandS, and the third row is the structure references.**

## 6 LIMITATIONS AND DISCUSSION

As shown in Figure 9, we have found that the refined results may be unsatisfactory in some cases. 1) In the first column, for specific styles, such as murals, our model might struggle to accurately capture the style of the hand, leading to alterations in texture details. 2) In the second column, our model may not accurately replicate the gloves onto the refined hands for hands-wearing gloves. 3) In the third column, hands holding objects may be unable to maintain their posture after refining. 4) In the fourth column, the hand mesh for structure guidance needs to be manually constructed for malformed hands that have difficulty reconstructing meshes automatically. Despite these limitations, our RHandS still provides a paradigm for refining malformed hands with decoupled structure and style guidance.

## 7 CONCLUSION

In this paper, we introduce a novel hand refining method RHandS. It decouples hand refining process into style guidance and structure guidance and employs a two-stage training strategy to fully leverage existing data and improve the structure of repainted hands as well as preserve the style in the original image. Furthermore, three datasets designed specifically for this task are built to facilitate research on multi-style hand refining. Qualitative and quantitative experiments demonstrate our method's superiority in adapting to images of various styles compared with existing methods.

## REFERENCES

- [1] Synthesis AI. [n. d.]. Static gestures dataset. <https://synthesis.ai/static-gestures-dataset/>.
- [2] Stability AI. 2022. Stable Diffusion Inpainting v1.5. <https://huggingface.co/runwayml/stable-diffusion-inpainting/>.
- [3] Stability AI. 2022. Stable Diffusion v1.5. <https://huggingface.co/runwayml/stable-diffusion-v1-5/>.
- [4] Shariq Farooq Bhat, Reiner Birkel, Diana Wofk, Peter Wonka, and Matthias Müller. 2023. Zoedepth: Zero-shot transfer by combining relative and metric depth. *arXiv preprint arXiv:2302.12288* (2023).
- [5] Xingyu Chen, Yufeng Liu, Yajiao Dong, Xiong Zhang, Chongyang Ma, Yanmin Xiong, Yuan Zhang, and Xiaoyan Guo. 2022. Mobrecon: Mobile-friendly hand mesh reconstruction from monocular image. In *Proceedings of the IEEE/CVF Conference on Computer Vision and Pattern Recognition*. 20544–20554.
- [6] MMPose Contributors. 2020. OpenMMLab Pose Estimation Toolbox and Benchmark. <https://github.com/open-mmlab/mmpose>.
- [7] Rinon Gal, Yuval Alaluf, Yuval Atzmon, Or Patashnik, Amit Haim Bermano, Gal Chechik, and Daniel Cohen-or. 2022. An Image is Worth One Word: Personalizing Text-to-Image Generation using Textual Inversion. In *The Eleventh International Conference on Learning Representations*.
- [8] Rohit Gandikota, Joanna Materzynska, Tingrui Zhou, Antonio Torralba, and David Bau. 2023. Concept sliders: Lora adaptors for precise control in diffusion models. *arXiv preprint arXiv:2311.12092* (2023).
- [9] Leon A Gatys, Alexander S Ecker, and Matthias Bethge. 2016. Image style transfer using convolutional neural networks. In *Proceedings of the IEEE conference on computer vision and pattern recognition*. 2414–2423.
- [10] Nicholas Guttenberg. 2023. Diffusion with offset noise.
- [11] Tiankai Hang, Shuyang Gu, Chen Li, Jianmin Bao, Dong Chen, Han Hu, Xin Geng, and Baining Guo. 2023. Efficient Diffusion Training via Min-SNR Weighting Strategy. In *IEEE/CVF International Conference on Computer Vision, ICCV 2023, Paris, France, October 1-6, 2023*. IEEE, 7407–7417. <https://doi.org/10.1109/ICCV51070.2023.00684>
- [12] Martin Heusel, Hubert Ramsauer, Thomas Unterthiner, Bernhard Nessler, and Sepp Hochreiter. 2017. Gans trained by a two time-scale update rule converge to a local nash equilibrium. *Advances in neural information processing systems* 30 (2017).
- [13] Jonathan Ho, Ajay Jain, and Pieter Abbeel. 2020. Denoising Diffusion Probabilistic Models. In *Advances in Neural Information Processing Systems 33: Annual Conference on Neural Information Processing Systems 2020, NeurIPS 2020, December 6-12, 2020, virtual*, Hugo Larochelle, Marc'Aurelio Ranzato, Raia Hadsell, Maria-Florina Balcan, and Hsuan-Tien Lin (Eds.). <https://proceedings.neurips.cc/paper/2020/hash/4c5bfc8584af0d967f1ab10179ca4b-Abstract.html>
- [14] Edward J Hu, Phillip Wallis, Zeyuan Allen-Zhu, Yuanzhi Li, Shean Wang, Lu Wang, Weizhu Chen, et al. 2021. LoRA: Low-Rank Adaptation of Large Language Models. In *International Conference on Learning Representations*.
- [15] Gabriel Ilharco, Mitchell Wortsman, Ross Wightman, Cade Gordon, Nicholas Carlini, Rohan Taori, Achal Dave, Vaishaal Shankar, Hongseok Namkoong, John Miller, Hannaneh Hajishirzi, Ali Farhadi, and Ludwig Schmidt. 2021. *OpenCLIP*. <https://doi.org/10.5281/zenodo.5143773>
- [16] Catalin Ionescu, Dragos Papava, Vlad Olaru, and Cristian Sminchisescu. 2013. Human3.6m: Large scale datasets and predictive methods for 3d human sensing in natural environments. *IEEE transactions on pattern analysis and machine intelligence* 36, 7 (2013), 1325–1339.
- [17] Xuan Ju, Ailing Zeng, Jianan Wang, Qiang Xu, and Lei Zhang. 2023. Human-art: A versatile human-centric dataset bridging natural and artificial scenes. In *Proceedings of the IEEE/CVF Conference on Computer Vision and Pattern Recognition*. 618–629.
- [18] Alexander Kapitanov, Karina Kvanchiani, Alexander Nagaev, Roman Kraynov, and Andrei Makhliarchuk. 2024. HaGRID–HAnd Gesture Recognition Image Dataset. In *Proceedings of the IEEE/CVF Winter Conference on Applications of Computer Vision*. 4572–4581.
- [19] Matthew Loper, Naureen Mahmood, Javier Romero, Gerard Pons-Moll, and Michael J Black. 2023. SMPL: A skinned multi-person linear model. In *Seminal Graphics Papers: Pushing the Boundaries, Volume 2*. 851–866.
- [20] Wenquan Lu, Yufei Xu, Jing Zhang, Chaoyue Wang, and Dacheng Tao. 2023. HandRefiner: Refining Malformed Hands in Generated Images by Diffusion-based Conditional Inpainting. *arXiv preprint arXiv:2311.17957* (2023).
- [21] Camillo Lugaresi, Jiuqiang Tang, Hadon Nash, Chris McClanahan, Esha Uboweja, Michael Hays, Fan Zhang, Chuo-Ling Chang, Ming Guang Yong, Juhyun Lee, et al. 2019. Mediapipe: A framework for building perception pipelines. *arXiv preprint arXiv:1906.08172* (2019).
- [22] Chenlin Meng, Yutong He, Yang Song, Jiaming Song, Jiajun Wu, Jun-Yan Zhu, and Stefano Ermon. 2022. SDEdit: Guided Image Synthesis and Editing with Stochastic Differential Equations. In *The Tenth International Conference on Learning Representations, ICLR 2022, Virtual Event, April 25-29, 2022*. OpenReview.net. [https://openreview.net/forum?id=aBsCjPu\\_tE](https://openreview.net/forum?id=aBsCjPu_tE)
- [23] Chong Mou, Xintao Wang, Liangbin Xie, Yanze Wu, Jian Zhang, Zhongang Qi, and Ying Shan. 2024. T2I-Adapter: Learning Adapters to Dig Out More Controllable Ability for Text-to-Image Diffusion Models. In *Thirty-Eighth AAAI Conference on Artificial Intelligence, AAAI 2024, Thirty-Sixth Conference on Innovative Applications of Artificial Intelligence, IAAI 2024, Fourteenth Symposium on Educational Advances in Artificial Intelligence, EAAI 2024, February 20-27, 2024, Vancouver, Canada*, Michael J. Wooldridge, Jennifer G. Dy, and Sriraam Natarajan (Eds.). AAAI Press, 4296–4304. <https://doi.org/10.1609/AAAI.V38I5.28226>
- [24] Alexander Quinn Nichol, Prafulla Dhariwal, Aditya Ramesh, Pranav Shyam, Pamela Mishkin, Bob McGrew, Ilya Sutskever, and Mark Chen. 2022. GLIDE: Towards Photorealistic Image Generation and Editing with Text-Guided Diffusion Models. In *International Conference on Machine Learning*. PMLR, 16784–16804.
- [25] Georgios Pavlakos, Vasileios Choutas, Nima Ghorbani, Timo Bolkart, Ahmed A. A. Osman, Dimitrios Tzionas, and Michael J. Black. 2019. Expressive Body Capture: 3D Hands, Face, and Body from a Single Image. In *Proceedings IEEE Conf. on Computer Vision and Pattern Recognition (CVPR)*.
- [26] Dustin Podell, Zion English, Kyle Lacey, Andreas Blattmann, Tim Dockhorn, Jonas Müller, Joe Penna, and Robin Rombach. 2023. SDXL: Improving Latent Diffusion Models for High-Resolution Image Synthesis. In *The Twelfth International Conference on Learning Representations*.
- [27] Alec Radford, Jong Wook Kim, Chris Hallacy, Aditya Ramesh, Gabriel Goh, Sandhini Agarwal, Girish Sastry, Amanda Askell, Pamela Mishkin, Jack Clark, et al. 2021. Learning transferable visual models from natural language supervision. In *International conference on machine learning*. PMLR, 8748–8763.
- [28] Aditya Ramesh, Prafulla Dhariwal, Alex Nichol, Casey Chu, and Mark Chen. 2022. Hierarchical text-conditional image generation with clip latents. *arXiv preprint arXiv:2204.06125*, 2 (2022), 3.
- [29] Robin Rombach, Andreas Blattmann, Dominik Lorenz, Patrick Esser, and Björn Ommer. 2022. High-resolution image synthesis with latent diffusion models. In *Proceedings of the IEEE/CVF conference on computer vision and pattern recognition*. 10684–10695.
- [30] Javier Romero, Dimitrios Tzionas, and Michael J. Black. 2017. Embodied hands: modeling and capturing hands and bodies together. *ACM Trans. Graph.* 36, 6 (2017), 245:1–245:17. <https://doi.org/10.1145/3130800.3130883>
- [31] Javier Romero, Dimitrios Tzionas, and Michael J. Black. 2017. Embodied Hands: Modeling and Capturing Hands and Bodies Together. *ACM Transactions on Graphics, (Proc. SIGGRAPH Asia)* 36, 6 (Nov. 2017).
- [32] Nataniel Ruiz, Yuanzhen Li, Varun Jampani, Yael Pritch, Michael Rubinstein, and Kfir Aberman. 2023. Dreambooth: Fine tuning text-to-image diffusion models for subject-driven generation. In *Proceedings of the IEEE/CVF Conference on Computer Vision and Pattern Recognition*. 22500–22510.
- [33] Chitwan Saharia, William Chan, Saurabh Saxena, Lala Li, Jay Whang, Emily L Denton, Kamyar Ghasemipour, Raphael Gontijo Lopes, Burcu Karagol Ayan, Tim Salimans, et al. 2022. Photorealistic text-to-image diffusion models with deep language understanding. *Advances in Neural Information Processing Systems* 35 (2022), 36479–36494.
- [34] ultralytics. 2022. YOLOv8. <https://github.com/ultralytics/ultralytics>.
- [35] Aaron Van Den Oord, Oriol Vinyals, et al. 2017. Neural discrete representation learning. *Advances in neural information processing systems* 30 (2017).
- [36] Zhenzhen Weng, Laura Bravo-Sánchez, and Serena Yeung. 2023. Diffusion-hpc: Generating synthetic images with realistic humans. *arXiv preprint arXiv:2303.09541* (2023).
- [37] Hu Ye, Jun Zhang, Sibio Liu, Xiao Han, and Wei Yang. 2023. Ip-adapter: Text compatible image prompt adapter for text-to-image diffusion models. *arXiv preprint arXiv:2308.06721* (2023).
- [38] Yufei Ye, Xueting Li, Abhinav Gupta, Shalini De Mello, Stan Birchfield, Jiaming Song, Shubham Tulsiani, and Sifei Liu. 2023. Affordance diffusion: Synthesizing hand-object interactions. In *Proceedings of the IEEE/CVF Conference on Computer Vision and Pattern Recognition*. 22479–22489.
- [39] Fan Zhang, Valentin Bazarevsky, Andrey Vakunov, Andrei Tkachenka, George Sung, Chuo-Ling Chang, and Matthias Grundmann. 2020. Mediapipe hands: On-device real-time hand tracking. *arXiv preprint arXiv:2006.10214* (2020).
- [40] Lvmin Zhang, Anyi Rao, and Maneesh Agrawala. 2023. Adding conditional control to text-to-image diffusion models. In *Proceedings of the IEEE/CVF International Conference on Computer Vision*. 3836–3847.
- [41] Shihao Zhao, Dongdong Chen, Yen-Chun Chen, Jianmin Bao, Shaozhe Hao, Lu Yuan, and Kwan-Yee K Wong. 2024. Uni-controlnet: All-in-one control to text-to-image diffusion models. *Advances in Neural Information Processing Systems* 36 (2024).
- [42] Zhuyi1997. [n. d.]. open-pose-editor. <https://github.com/Zhuyi1997/open-pose-editor>.
- [43] Christian Zimmermann and Thomas Brox. 2017. Learning to Estimate 3D Hand Pose from Single RGB Images. In *IEEE International Conference on Computer Vision, ICCV 2017, Venice, Italy, October 22-29, 2017*. IEEE Computer Society, 4913–4921. <https://doi.org/10.1109/ICCV.2017.525>

## A SUPPLEMENTARY DETAILS

In this supplementary material, we show the details of our proposed multi-style datasets, a further quantitative evaluation through a user study, and more hand refining results.

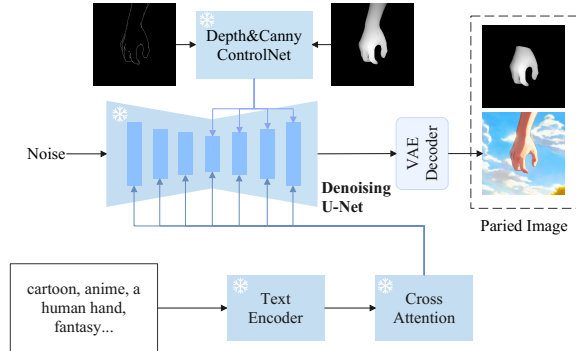


**Figure 10: The constructing process of our multi-style hand-mesh dataset for the 2nd training stage.**

### A.1 Details of Multi-Style Dataset

In this subsection, we introduce details about the constructing process and statistics of our multi-style hand-mesh dataset for the second training stage and multi-style malformed hand-mesh dataset for evaluation, respectively.

**A.1.1 Multi-Style Hand-Mesh Dataset.** Figure 10 shows the constructing process of our multi-style hand-mesh dataset. We combine SMPL-H model [31] and stable diffusion model [29] to synthesize the multi-style hand-mesh dataset. We first use SMPL-H model to generate 3d human models with random shapes, hand poses, and body poses. Specifically, we sample the shape and hand pose parameters from random normal distributions and generate the body pose parameters using vposer [25]. Then, we crop out the hand region from the full human mesh and use a camera with a field-of-view of 45 degrees to render the hand depth images with and without an arm, respectively. Next, We extract canny images from the hand depth images with an arm and feed them into pre-trained canny and depth ControlNet [40] to guide the structure generation. To synthesize hand images of various styles, we manually customize the text prompt for each style to guide the generation process to match each target style. We finally synthesized 10K images for a totaling 7 styles (natural human, oil painting, watercolor, cartoon, sculpture, digital art, garage kit) and filtered out 20% images for each style using the MPJPE metric introduced in the main material. Beyond this, we further collect, crop, and resize 18962 images from SGD dataset [1] as one extra 3d rendering style. Figure 11 shows the training dataset examples of the above 8 styles used in stage 2.

**A.1.2 Multi-style Malformed Hand-Mesh Dataset.** Figure 12 shows the constructing process of our multi-style malformed hand-mesh dataset. We use the HumanArt dataset [17] as a reference to construct our dataset for evaluation. Specifically, we first detect, crop, and resize hands from each original image. Then, we employ MoBRecon [5] to reconstruct hands from the hand images and manually

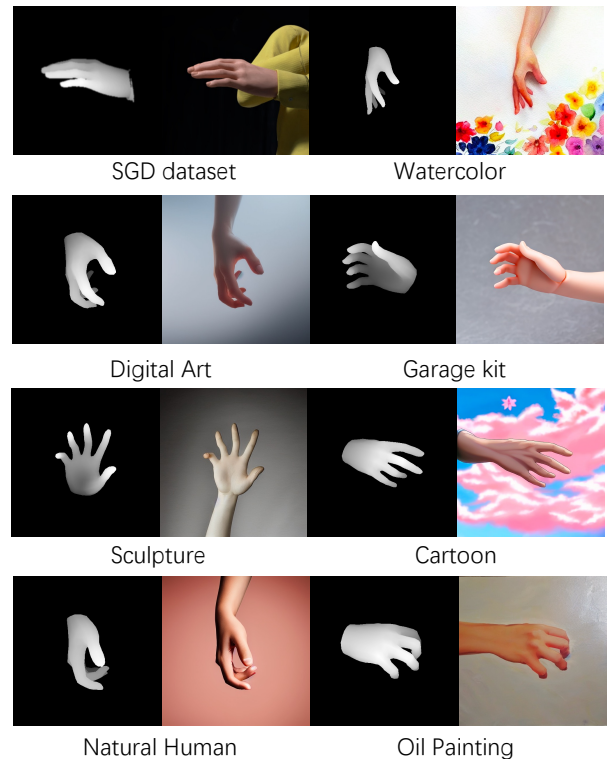


**Figure 11: Examples of multi-style hand-mesh training dataset for the 2nd training stage.**

filter out images of badly reconstructed hands. Finally, we use the stable diffusion inpainting model [2] to repaint the center region of each hand to get the corresponding malformed hand image. The HumanArt dataset has human body images of 20 categories, and after filtering, we got 18 categories, totaling 1440 hand images to construct our dataset. The number of images for each style are: 209 dance, 70 watercolor, 38 stained glass, 86 movie, 46 acrobatics, 306 cosplay, 77 sculpture, 112 drama, 86 digital art, 21 shadow play, 51 mural, 24 sketch, 3 kids drawing, 121 oil painting, 26 ink painting, 52 cartoon, 76 garage kits, 36 relief.

### A.2 Quantitative Evaluation with User Study

To further evaluate our RHandS with current state-of-the-art methods, we add a user study to conduct the subjective comparison with HandRefiner [20]. We uniformly sample 173 image pairs (3 for kids drawing and 10 for each other style) from our multi-style malformed hand-mesh dataset and show the image pairs of the malformed hand, the hand refined with HandRefiner, and the hand refined with RHandS to users side-by-side. We ask users to select the preferred hand image with better structure and style consistency following logic shown in Algorithm 1. This logic considers style consistency first and then compares the structure quality of different methods. If refined images of HandRefiner and RHandS show both bad style consistency and malformed hand structure, users would reject the two methods and select “None” as the final option.

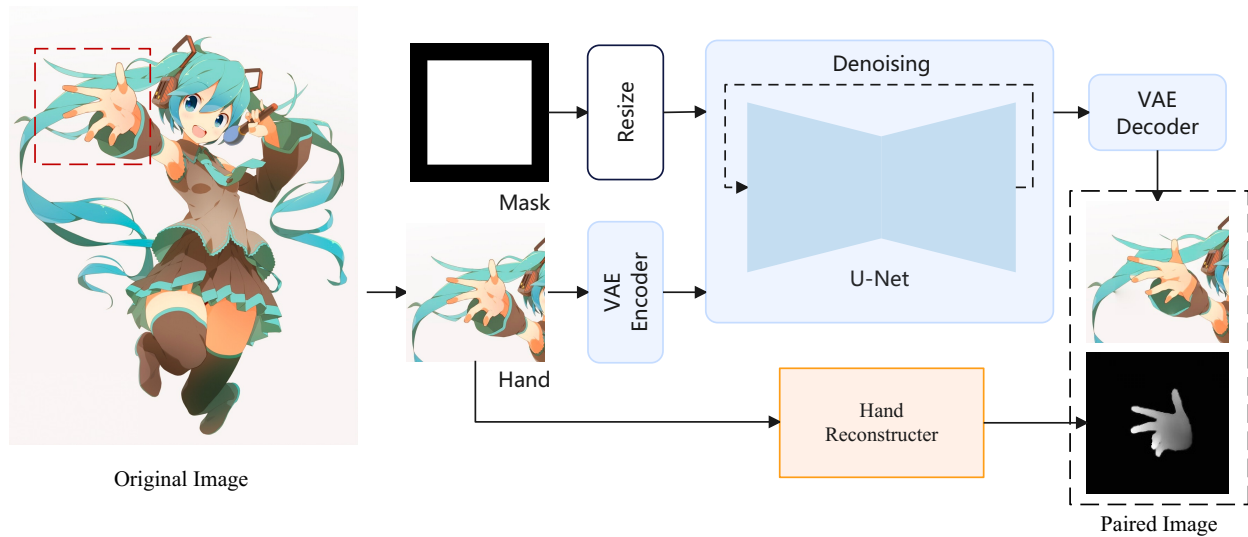


Figure 12: The constructing process of our multi-style malformed hand-mesh for evaluation.

**Algorithm 1: Human evaluation logic**

```

Input: malformed hand image  $I_1$ , refined image of
    HandRefiner  $I_2$ , refined image of RHandS  $I_3$ 
Output: preferred image  $I$ 
if style of  $I_2$  is consistent with  $I_1$  and style of  $I_3$  is consistent
    with  $I_1$  then
    |  $I \leftarrow$  one of  $\{I_2, I_3\}$  with better hand structure
else
    |  $I' \leftarrow$  one of  $\{I_2, I_3\}$  with better style consistency
    |  $I'' \leftarrow$  one of  $\{I_2, I_3\}$  with worse style consistency
    if  $I'$  has good hand structure then
    |  $I \leftarrow I'$ 
    else
    | if  $I''$  has good hand structure then
    | |  $I \leftarrow I''$ 
    | else
    | |  $I \leftarrow \text{None}$ 
    | end
    end
end
    
```

Figure 13 shows the statistics of most human preferences on the three categories for each image pair. For natural human styles (acrobatics, cosplay, dance, drama, movie), the final selection distribution of HandRefiner, RHandS, and None is 8, 37, 5. And for artificial human styles (garage kits, relief, sculpture, kids drawing, mural, oil painting, shadow play, sketch, stained glass, cartoon, digital art, ink painting, and watercolor), the final preference distribution is 17, 72, 34. Only for one extreme style of shadow play, both HandRefiner and RHandS failed to refine malformed hands with appropriate style and structure, and most users select “none” (1, 0, 9). Despite that, users prefer our RHandS over most other styles. These results validate the conclusion that our method can refine malformed hands with more style consistency and structure quality.

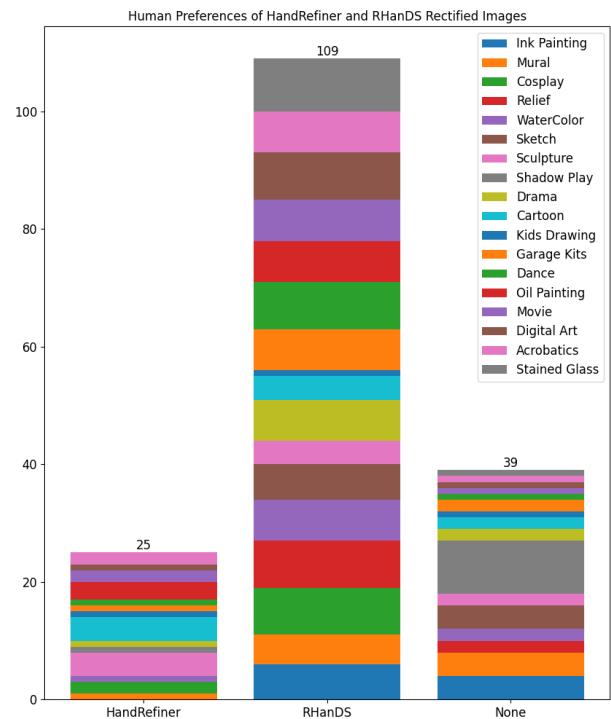


Figure 13: Visual results of user study evaluation.

**A.3 Further Examples**

In this subsection, we show more refining examples of RHandS to demonstrate the general adaption ability of our method. Figure 14 shows the results.

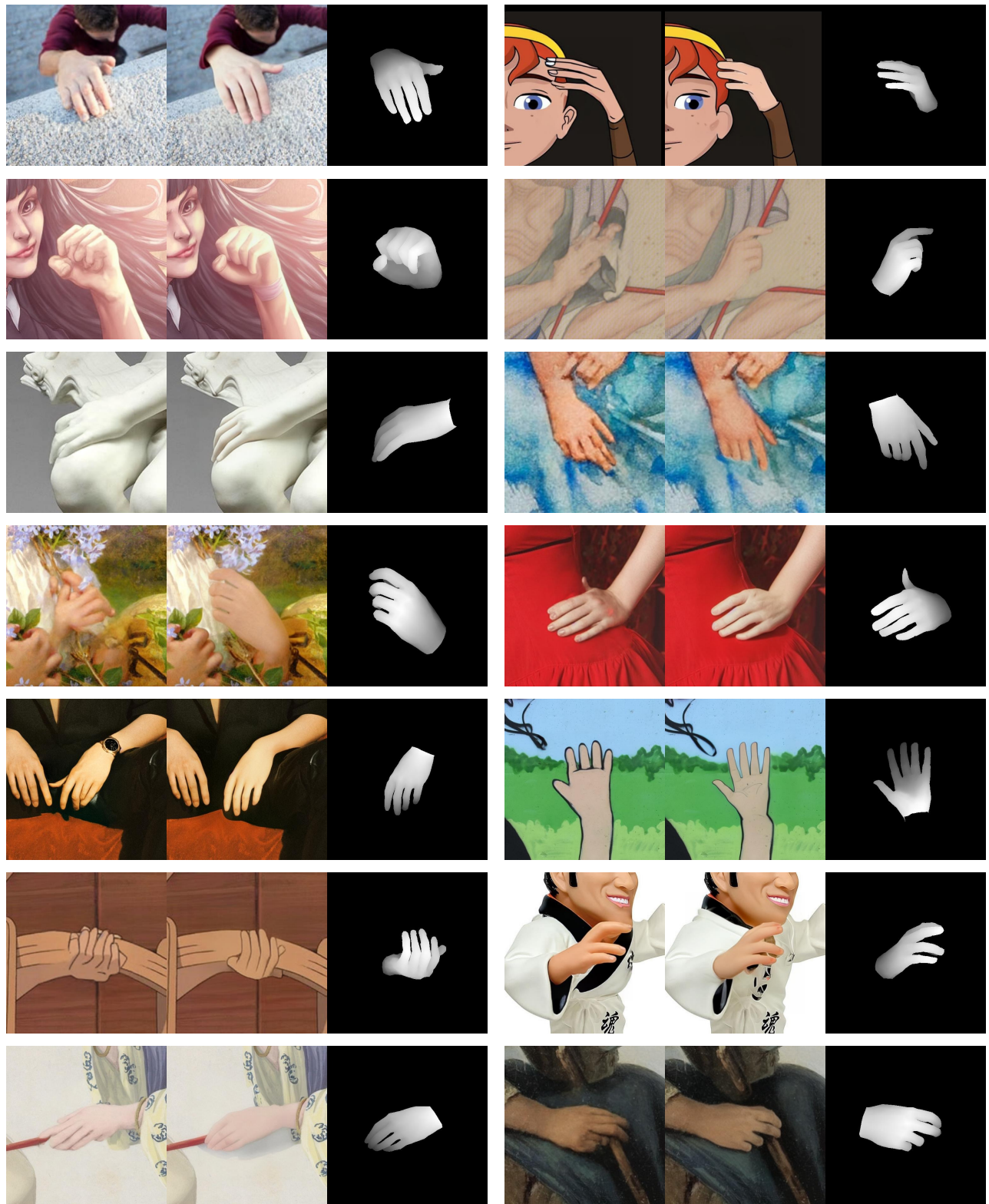


Figure 14: More refining examples of our RHandS. In each image pair, the malformed hand, refined hand, and corresponding structure guidance are presented sequentially from left to right.